Strengthening of reinforced concrete corbels with GFRP overlays

Sevket Ozden and Hilal Meydanli Atalay*

Department of Civil Engineering, Kocaeli University,
Kocaeli 41040, Turkey,
e-mail: hilal.meydanli@kocaeli.edu.tr

*Corresponding author

Abstract

The strength and post-peak performance of reinforced concrete corbels, strengthened with epoxy bonded glass fiber reinforced polymer (GFRP) overlays, were experimentally investigated. The test variables were the corbel shear span to depth ratio, corbel main reinforcement ratio, and the number and orientation of the GFRP fibers. In total, 24 normal strength concrete, one-third scale, corbel specimens, without hoop reinforcement, were tested to failure under quasi-static gravity loading. Test results revealed that GFRP overlays can easily be used for the enhancement of corbel load bearing capacity, depending on the fiber orientation. The main reinforcement ratio and the number of GFRP plies were found to be the two main variables affecting the level of strength gain in the corbel specimens.

Keywords: corbel; glass fiber reinforced polymer; normal strength concrete; reinforced concrete, strengthening.

Notation

a/d, shear span to depth ratio; b, width of corbel (mm); d, effective corbel depth on the corbel-column interface (mm); f_c', compressive strength measured on 150×300 mm concrete cylinders (MPa); f_{sp}, split tensile strength measured on 150×300 mm concrete cylinders (MPa); f_y, yield strength of corbel main reinforcement or column longitudinal reinforcement (MPa); f_{yw}, yield strength of column transverse reinforcement (MPa); h', the corbel depth on the outer edge of the bearing area (mm); h, the corbel height (mm); H, horizontal load on the corbel (kN); H/V, horizontal load to vertical ratio; P, applied load on the column ($V_u = P/2$) (kN); V, vertical load on the corbel (kN); V_u, vertical failure load of a corbel ($V_u = P/2$) (kN); ε_D, corbel concrete strain measured on 45 degree inclination with the horizontal (Figure 3); ε_L, corbel concrete strain measured parallel to the corbel main reinforcement (Figure 3); Φ, prefix for reinforcing bar diameter in millimeters; ρ, main reinforcement ratio measured on the corbel-column cross-section (%); τ, shear stress of the a corbel (MPa).

1. Introduction

Reinforced concrete cantilever beams with shear span to effective depth ratios (a/d) less than unity are usually named corbels, and their response under gravity loads significantly differs from that of the beams with higher ratios of a/d. Corbels are mainly in the form of overhanging beams or beams protruding from the column faces which are used either to support the other structural members or to support the crane loads at industrial buildings. In either case, the structural integrity is closely related to the strength and post-peak response of the corbels.

Corbels were generally designed for gravity loads only, although the horizontal forces could be invoked either owing to restrained creep, shrinkage or temperature deformations which takes place in the supported members. The behavior of reinforced concrete corbels is mainly influenced by the type of loading, the shear span to effective depth ratio, the concrete strength, type, amount and orientation of the reinforcement, and the corbel geometry. Some studies showed that corbels tend to fail in several modes because of these various parameters. The failure modes can vary from being sudden and catastrophic to gradual and more ductile [1–3].

Kriz and Raths [1] reported the first extensive research, experimental and analytical, on strength and response properties of reinforced concrete corbels, concluding with the design criterion and capacity prediction equations. A large number of corbel specimens of the research was subjected to vertical loads only, whereas some specimens were subjected to a combination of vertical and horizontal loads. According to Kriz and Raths, failure modes of tested specimens are classified into two fundamental groups, namely principle and secondary modes. Principle modes of failure were flexural tension, flexural compression, diagonal splitting, and the shear failure. Secondary modes of failure were the corbel non-loaded end failure, bearing failure under steel loading plate, and the crack intersecting the sloping face of the corbel. It is reported that the tension reinforcement and horizontal stirrups are likewise effective in increasing the strength of corbels subjected to vertical loads only [1].

Mattock et al. [4] reported the design criterion for the horizontal stirrup reinforcement in the corbels. The variables included in this study were the shear span to effective depth ratio (a/d), the horizontal to vertical load ratio (H/V), the tension reinforcement ratio (ρ), the amount of stirrup reinforcement, and the type of aggregate. Test results revealed that the corbels without stirrups underwent brittle failure through complete diagonal tension failure. It was reported that the minimum stirrup reinforcement will prevent premature diagonal tension failures in corbels, hence permitting the yield strength of the tension reinforcement to be developed. It was also reported that the tension reinforcement yields before the failure of corbels; in the case of low values of a/d and low values of tension reinforcement ratios [4].

Fattuhi [5] and Fattuhi and Hughes [6] reported that the ultimate load capacity and the ductility of reinforced concrete corbels are improved by the addition of steel fiber reinforcement (SFR). Ductility in this study referred to the ability of a corbel to undergo large deformations after reaching the ultimate load without suffering much loss in load carrying capacity or exhibiting a sudden fracture [6]. Whereas the influence of SFR on ultimate load capacity of corbels subjected to vertical loading was investigated initially, the subsequent studies investigated the influence of type and geometry of the SFR itself, when the corbels were subjected to various combinations of horizontal and vertical loads [7–9]. Abdul-Wahab [10] reported that the addition of SFR to concrete resulted in an overall improvement in the performance of corbels by acting as crack arrestors, and by yielding an improved energy absorption capacity [10].

The effect of using high strength concrete (HSC) in corbels subjected to vertical loads or combined loading was also investigated and reported by researchers [11–13]. The extent of crack for high strength concrete corbels is almost the same as normal strength concrete corbels, and HSC corbel behavior was similar to normal strength ones when failure took place after yielding the main reinforcement [12]. It is reported that the increase in concrete strength generally leads to an increase in the corbel load bearing capacity, but does not result in brittle failure and does not affect the corbel ductility. By contrast, the increase in the reinforcement ratio in HSC corbels increases the strength, while decreasing the ductility at failure [12]. In existence of secondary reinforcement, such as stirrups, HSC corbels experience reduced crack widths and improved ductility and the failure is through the crushing of the compression strut [13]. It is reported that the first flexural cracking load decreases with an increase in the shear span to effective depth ratio [13].

In recent years, the use of fiber reinforced plastics in strengthening the existing structures became popular all around the world and significant research was initiated on every aspect of the topic [14, 15].

Elgwady et al. [16] reported that the external strengthening of a corbel using effectively arranged laminated carbon fiber reinforced polymers (CFRPs) can enhance the corbel capacity. Corbels upgraded with CFRP laminates showed a brittle mode of failure and failed suddenly without adequate warning because of the increased stiffness of the corbels and the sudden debonding of the CFRP laminate layers. It is also reported that the stress in the CFRP strips at the time of corbel failure was significantly less than the ultimate capacity of CFRP owing to the debonding type of failure of the CFRP strips and owing to the spalling of concrete cover [16].

The flexural behavior of reinforced concrete corbels was also investigated by Campione et al. [17]. By evaluating the behavior of specimens having the same shape and dimension, they compared the effect of traditional steel reinforcement with the SFR and the externally wrapped CFRP. It is concluded that the flexural capacity of corbels was increased by adding SFR or wrapping CFRP [17].

In the present study, the results of an experimental study on the flexural behavior of strengthened reinforced corbel through externally wrapped glass fiber reinforced polymer (GFRP) are presented. The objective of the research was to increase the load bearing capacity, while avoiding a brittle post-peak response.

2. Materials and methods

Substandard design and/or poor construction stages, increasing crane loads, or changing loads and load combinations can increase the need of a rational and rapid strengthening method for reinforced concrete corbels. Among many other methods, the use of GFRP overlays is considered as an effective way for the strengthening of corbels within the scope of the current experimental investigation.

In total, 24 normal strength concrete corbels (f_c'=23–26 MPa) were constructed without stirrups, to simulate the on-site inferior conditions. Three tension reinforcement ratios (ρ_1=0.45%, ρ_2=0.89%, ρ_3=1.40%) were used in the corbel specimens, and two GFRP fiber orientations (lateral and diagonal) were investigated. One and three layers were used in the diagonal GFRP application, whereas three layers were used in the lateral GFRP application. The corbel specimens were tested under two different shear span to depth ratios (a/d=0.40, a/d=0.80). The test was performed under monotonically increasing vertical load (shear), while the horizontal component of the load was set to zero.

2.1. Test specimens

The test specimens consisted of reinforced concrete corbels classified into three main groups according to the main reinforcement ratio as shown in Figure 1. The main reinforcement for the first group of corbel specimens (namely the group HC1) was a single 8 mm diameter (Φ8) deformed reinforcing steel bar, whereas it was two Φ8 bars for the second corbel group (group HC2). Two 10 mm diameter (Φ10) deformed bars were used as main reinforcement in the third set of specimens (group HC3). No hoop reinforcement was used in either of the specimen sets.

Each specimen consists of a column with two corbels arranged symmetrically on both sides of the column, and all corbels have the same dimensions as shown in Figure 1. The cross-sectional dimensions of the 420 mm long rectangular column were 75 mm by 150 mm, and four 8 mm diameter deformed bars were used as column longitudinal reinforcement, whereas 6 mm diameter plain bars at a spacing of 60 mm were used as hoop reinforcement. In all specimens, the width of corbels was b=75 mm, and the height was h=170 mm, resulting an effective depth of d=150 mm. The depth at the outer edge of the bearing area was h'=95 mm.

The specimen designation can be interpreted as follows: the first three letters represents the group names ("HC1" for the first group, "HC2" for the second group, and "HC3" for the third group), in return indicating the main reinforcement ratios. The main reinforcement ratio for the HC1 specimen group was ρ=0.45%, and the reinforcement ratios for specimen groups HC2 and HC3 were ρ=0.89% and ρ=1.40%,
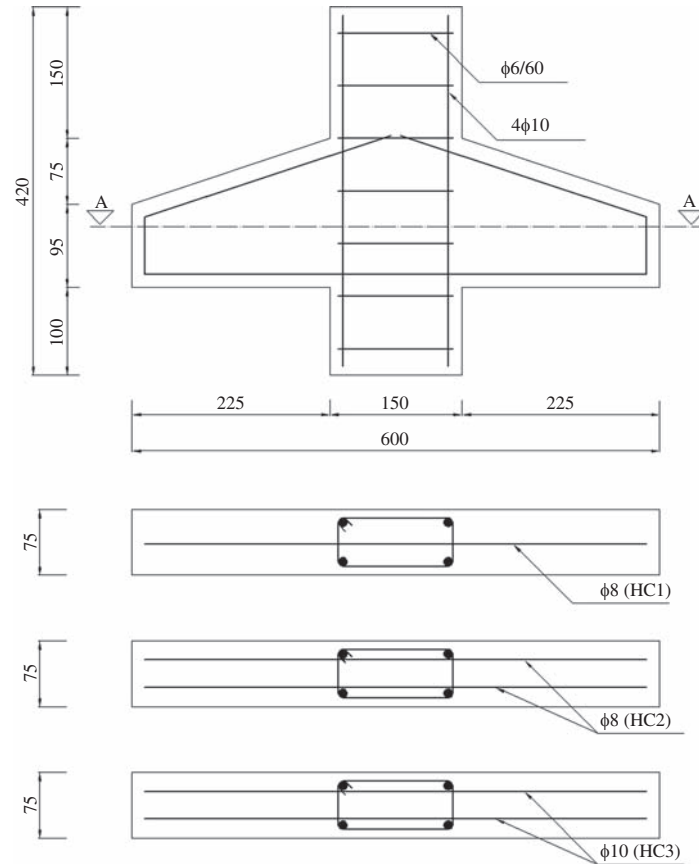
Figure 1   Reinforcement detail of corbel specimens (units are mm).

respectively. The shear span to depth ratio (*a/d*) of the specimens were shown in the next field of the specimen name; 40 for *a/d*=0.40 and 80 for *a/d*=0.80. The last three letters in the specimen names represents the number of glass fiber layers and directions applied to the corbels (H: horizontal, D: diagonal). Specimen name HC240F00 represents the non-strengthened specimen with a main reinforcement ratio of *ρ*=0.89%, loaded at a shear span to depth ratio of *a/d*=0.40, whereas HC240F3D represents the counterpart specimen strengthened with three layers of GFRP applied diagonally on both sides of the corbel.

2.2. Material properties

The physical and mechanical properties of the GFRP and the mechanical properties of epoxy resin used in the strengthened specimens are given in Table 1. It should be noted that these values are producer specified values and equal volumetric ratios between GFRP and the epoxy were used during the impregnation of the GFRP in this experimental investigation.

Identical concrete mix design proportions with the same ingredients were used for all specimens in order to flatten the probable material effects on member response. The concrete compressive (f_c') and split tensile (f_{sp}) strength values attained at the time of specimen tests are listed in Table 2. The con-

crete compressive strength and split cylinder strength values were measured on 150×300 mm cylinders.

The yield strength of deformed column longitudinal reinforcement (*Φ*10) and plain column transverse reinforcement (*Φ*6) were f_y=452 MPa and f_{yw}=230 MPa, respectively. The yield (f_y) and the ultimate strength (f_u) values of 8 mm and 10 mm diameter reinforcing bars used as corbel tension reinforcement are given in Table 2.

2.3. Strengthening of specimens

GFRP wraps with different number of layers and with different orientations were used in strengthening of the corbel specimens (Figure 2). One and three layer patterns for

**Table 1**   Mechanical properties of GFRP and epoxy.

Property	GFRP	Epoxy
Design thickness (mm)	0.157	N/A
Modulus of elasticity (MPa)	73,000	6000
Tensile strength (MPa)	3400	17
Compressive strength (MPa)	N/A	80
Flexural tensile strength (MPa)	N/A	30
Fiber density (g/m³)	2.54	N/A
Fiber areal weight (primary/transverse) (g/m²)	400/40	N/A
Ultimate elongation (%)	4.66	N/A

Table 2 Corbel material properties and test results.

Specimen	Concrete		Steel		a/d	ρ (%)	GFRP		V_u (kN)	τ	$\Delta\tau$ (w.r.t. control spc.)
	f'_c (MPa)	f_{sp} (MPa)	f_y (MPa)	f_u (MPa)			# of layers	Orientation			
HC140F00	23	2.47	452	667	0.40	0.45	0	N/A	63	1.16	–
HC140F1D	23	2.47	452	667	0.40	0.45	1	Diagonal	98	1.81	0.65
HC140F3D	23	2.47	452	667	0.40	0.45	3	Diagonal	133	2.46	1.30
HC140F3H	23	2.47	452	667	0.40	0.45	3	Lateral	81	1.50	0.33
HC180F00	23	2.47	452	667	0.80	0.45	0	N/A	49	0.90	–
HC180F1D	23	2.47	452	667	0.80	0.45	1	Diagonal	71	1.31	0.41
HC180F3D	23	2.47	452	667	0.80	0.45	3	Diagonal	74	1.36	0.46
HC180F3H	23	2.47	452	667	0.80	0.45	3	Lateral	45	0.83	N/A
HC240F00	26	2.65	512	738	0.40	0.89	0	N/A	85	1.49	–
HC240F1D	26	2.65	512	738	0.40	0.89	1	Diagonal	125	2.19	0.70
HC240F3D	26	2.65	512	738	0.40	0.89	3	Diagonal	166	2.91	1.41
HC240F3H	26	2.65	512	738	0.40	0.89	3	Lateral	84	1.47	N/A
HC280F00	26	2.65	512	738	0.80	0.89	0	N/A	63	1.10	–
HC280F1D	26	2.65	512	738	0.80	0.89	1	Diagonal	92	1.60	0.51
HC280F3D	26	2.65	512	738	0.80	0.89	3	Diagonal	105	1.84	0.73
HC280F3H	26	2.65	512	738	0.80	0.89	3	Lateral	71	1.24	0.14
HC340F00	25	2.84	451	718	0.40	1.40	0	N/A	86	1.54	–
HC340F1D	25	2.84	451	718	0.40	1.40	1	Diagonal	119	2.14	0.59
HC340F3D	25	2.84	451	718	0.40	1.40	3	Diagonal	148	2.65	1.10
HC340F3H	25	2.84	451	718	0.40	1.40	3	Lateral	77	1.37	N/A
HC380F00	25	2.84	451	718	0.80	1.40	0	N/A	45	0.80	–
HC380F1D	25	2.84	451	718	0.80	1.40	1	Diagonal	111	1.98	1.17
HC380F3D	25	2.84	451	718	0.80	1.40	3	Diagonal	139	2.49	1.67
HC380F3H	25	2.84	451	718	0.80	1.40	3	Lateral	64	1.14	0.34

$\tau = V_u/(b \times d \times \sqrt{f'_c})$.

diagonal GFRP wrapping (45 degrees with the horizontal) was applied (Figure 2), whereas only three layer pattern was used for horizontal GFRP configuration. The GFRP sheets were applied on fully cured, surface-dry specimens with rounded corners. The residue on corbel surface was removed and aggregates were exposed by using bush hammering and vacuum cleaner before the GFRP wrapping was applied. The GFRP strips were cut to the predetermined width and length by using an ordinary pair of scissors and their surface was kept clean by using a cotton brush. A two component epoxy (resin and hardener) was mixed, weighed and applied to the concrete surface and GFRP sheets concurrently, within the producer specified pot-time. Finally, the coated sheets were wrapped to the specimens and aluminum rollers were used for even bonding of GFRP to the concrete surface.


Diagonal   Lateral
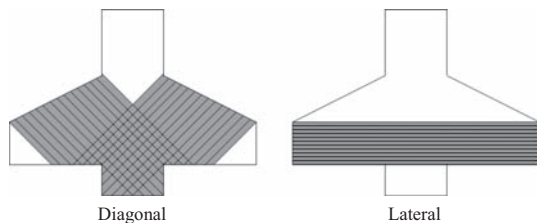
Figure 2 GFRP wrapping configurations.

2.4. Loading and instrumentation

All test specimens were white washed before the test in order to trace the crack patterns and loaded under a 1300 kN capacity rigid frame by using a 600 kN capacity load controlled, manually driven hydraulic actuator (Figure 3). The vertical load (gravity load in real) which was applied onto the column via a roller support and measured by a 600 kN capacity electronic load cell. It was assumed that the vertical load is equally divided between two protruding corbels as shown in Figure 3. The test specimens, which were inverted columns with two protruding corbels, were seated on two roller supports, resulting in a horizontal to vertical load ratio (H/V) of zero on corbels.

The corbels were seated on roller supports at distances of 60 mm and 120 mm from the column face, yielding a/d ratios of 0.40 and 0.80. The vertical load P, hence the shear force on corbel ($P/2$), was increased monotonically until the shear failure load of the corbel (V_u) on either side of the specimen is reached. The failure is defined as the sudden and excessive loss of load bearing capacity of the test specimen. After each load increment the development of cracks was observed and marked on the specimens.

The concrete strains in the diagonal (ε_D) and lateral directions parallel to the main reinforcement (ε_L) were measured and recorded electronically throughout the loading scheme (Figure 3). It should be noted that the diagonal (ε_D) and lateral
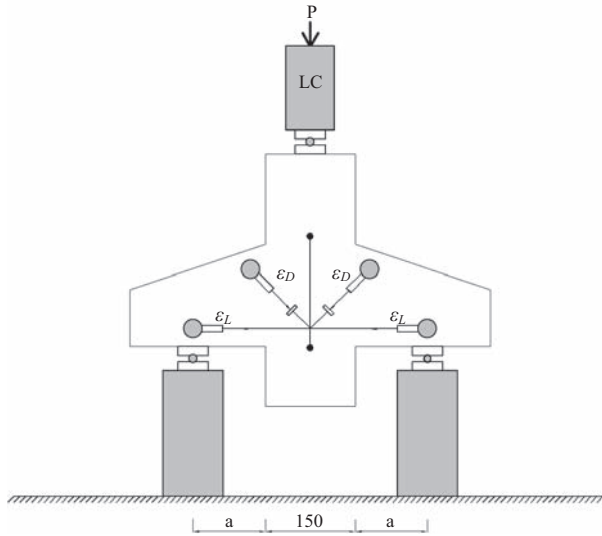
Figure 3 Loading set-up and deformation measuring device locations (units are mm).

(ε_L) strains were also measured on strengthened specimens and these values were considered to calculate the GFRP stress level attained at the time of ultimate shear force, V_u.

3. Results and discussion

In this section, the observed behavior and modes of failure for each specimen will be described. Material properties and the maximum load carried by each corbel are listed in Table 2. The failure mode of each corbel is shown in Figure 4. The crack patterns were changed relative to the configuration of GFRP overlays, reinforcement ratios, and the *a/d* ratios. The thorough examination and the proper understanding of the crack patterns have prime importance on the predetermination of the best GFRP orientation.

3.1. Improvement in failure loads

Test results revealed that the load capacity of the corbels was increased by externally bonded GFRP overlays (Table 2). The level of strengthening depends on all variables of the current investigation, which are the reinforcement ratio, *a/d* ratio, and the orientation and number of layers of the GFRP overlays. For *a/d*=0.40, the effectiveness of the GFRP with single layer decreased with increasing reinforcement ratio. For the HC1 set (ρ=0.45%) the strength increase was 56%, whereas the same amount of GFRP resulted in an increase of 39% for the specimen having ρ=1.40% (HC3 set). It should be noted that the strength increase for the set HC2 specimen (r=0.89%) was 47%. Keeping *a/d* ratio the same, the use of three layers of diagonal GFRP resulted in 112%, 98%, and 72% capacity increases for specimens having ρ=0.45%, ρ=0.89%, and ρ=1.40%, respectively (Figure 5).

When the *a/d* ratio is 0.80, in contrast to *a/d*=0.40, the effectiveness of the diagonal GFRP overlays increases with

increasing reinforcement ratio. Single layer of diagonal GFRP resulted in 31%, 41%, and 147% increase for specimens with low, medium, and high reinforcement ratios, whereas three GFRP layers resulted in 37%, 91%, and 212% load capacity increases for the counterpart specimens (Figure 6).

The effect of horizontal GFRP overlays on the load capacity enhancement is more fluctuating. Whereas a small increase in capacity is observed for the specimen with *a/d*=0.40 for low reinforcement ratio, no capacity increase is observed for medium and high reinforcement ratios. By contrast, the capacity increase is approximately between 10% and 40% for specimens with *a/d*=0.80, regardless of the reinforcement ratio.

3.2. Average concrete shear strain vs. normalized shear stress behavior

The average concrete strains in diagonal (ε_D) and lateral (ε_L) directions (Figure 3) were measured during the testing of control and strengthened corbels. It was observed that the normalized shear stress [$\tau=V/(b\times d\times\sqrt{f'_c})$] vs. the average concrete strain (ε_L or ε_D) response for all specimens yields similar behavior as shown in Figure 7. The first point of change in slope of the response (τ_1-ε_{1L} or τ_1-ε_{1D}) usually corresponds to the point where the first flexural crack on the corbel-to-column boundary is observed. The second point of change in the slope (τ_2-ε_{2L} or τ_2-ε_{2D}) usually indicates the development of a shear crack, whereas the failure point or the point where the test is terminated is marked as τ_3-ε_{3L} or τ_3-ε_{3D}. The stress and the corresponding strain values of specimens, as illustrated in Figure 7, are given in Table 3.

It is observed that the concrete normalized shear stress at first flexural cracking τ_1 changes with the *a/d* ratio of the specimen, the smaller the *a/d* ratio, the higher the τ_1 values, as expected. By contrast, the enhancement of τ_1 through the application of GFRP overlays is more pronounced for specimens with higher reinforcement values (Table 3). The application of diagonal GFRP overlay with regard to the corresponding control specimen resulted in approximately no increase in the τ_1 values of the HC1 set of specimens, whereas the increase in the HC3 set of specimens was in the range of 25–50%. A similar trend is observed for the τ_2 values. The average concrete strains reached at the onset of the shear cracking and at the point of failure are very much affected by the existence of the diagonally applied GFRP overlays, higher numbers of layers result in higher percent of increases. By contrast, the applications of lateral GFRP overlays negatively affect the attained stresses, especially the strains, both at the onset of the shear cracking and at the failure point.

The measured normalized shear stress vs. concrete average strain in the predefined directions (ε_L and ε_D) for each corbel is given in Figure 8. It should be noted that the direction of the lateral strain measurements (ε_L) coincide with the direction of the corbel main reinforcement, whereas the diagonal average concrete strains (ε_D) were measured on a slope of 45 degrees inclined with regard to the corbel main reinforcement, hence parallel to the fibers of the diagonally wrapped specimens.
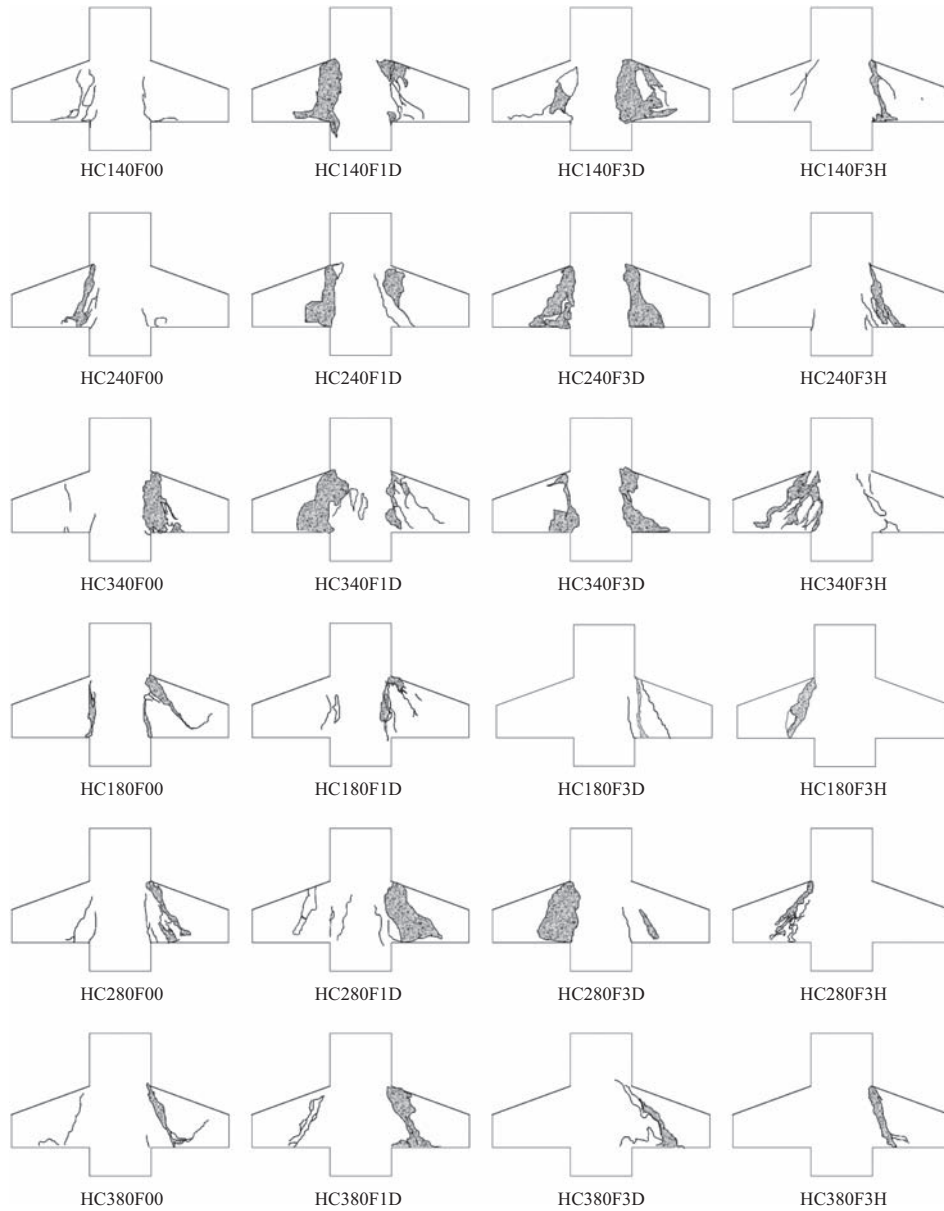
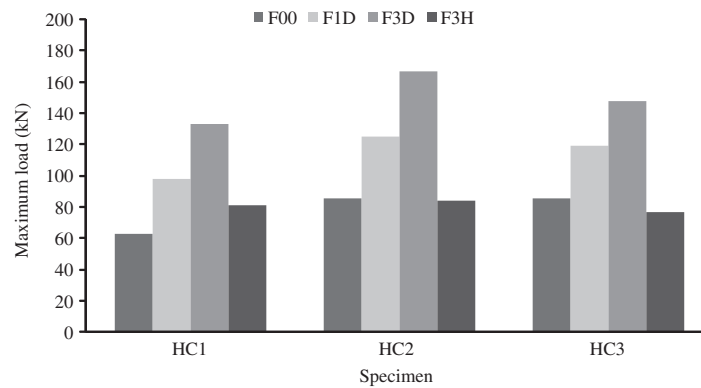**Figure 4**   Crack pattern for corbel specimens.

Figure 5   Maximum loads vs. strengthening configurations for *a*/*d*=0.40.
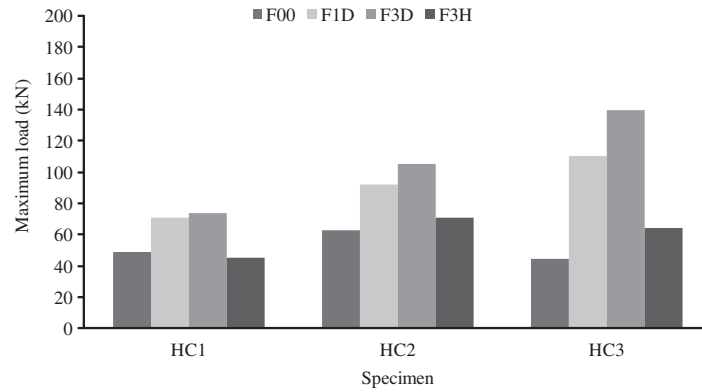
Figure 6 Maximum loads vs. strengthening configurations for *a/d*=0.80.
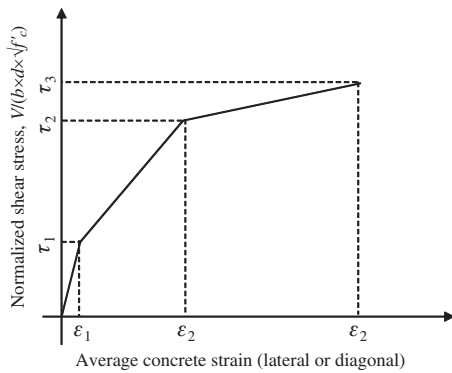

Figure 7 Illustration of the specimen response.

The state of yielding of the main reinforcement at the time of ultimate load level is anticipated through the ε_{3L} readings. Although the ε_{3L} readings are in the direction of the main reinforcement, it should be noted that the measured values are solely average concrete strains. The anticipated steel strain at the time of first flexural cracking at corbel-to-column interface is approximately 5–10% of the yield. The data in Table 3 also reveal that the anticipated steel strains of the strengthened corbels (diagonal GFRP) are far less than the yield at the onset of shear cracking, especially for specimens with low *a/d* values. By contrast, the main reinforcement seems yielding or very close to yielding for higher *a/d* ratios for the similar diagonal GFRP applications. The anticipated steel strains at the time of failure for the strengthened corbels with diagonal

Table 3 Normalized shear stress and average concrete strain values with regard to Figure 5 illustrations.

Specimen	$\tau=V/(b\times d\times\sqrt{f'_c})$			ε lateral ($\times10^{-3}$)			ε diagonal ($\times10^{-3}$)			$\varepsilon_{1L}/\varepsilon_y$	$\varepsilon_{2L}/\varepsilon_y$	$\varepsilon_{3L}/\varepsilon_y$
	τ_1	τ_2	τ_3	ε_{1L}	ε_{2L}	ε_{3L}	ε_{1D}	ε_{2D}	ε_{3D}			
HC140F00	0.44	1.04	1.17	0.066	1.308	3.067	0.147	0.844	4.041	0.03	0.58	1.36
HC140F1D	0.44	1.60	1.81	0.066	1.631	3.190	0.147	2.349	4.794	0.03	0.72	1.41
HC140F3D	0.88	2.19	2.43	0.069	1.837	4.495	0.584	3.728	9.279	0.03	0.81	1.99
HC140F3H	0.44	1.49	1.49	0.066	1.429	1.429	0.147	1.095	1.095	0.03	0.63	0.63
HC180F00	0.25	0.59	0.90	0.258	1.202	11.84	0.038	2.022	13.52	0.11	0.53	5.24
HC180F1D	0.25	1.00	1.31	0.258	2.497	11.071	0.038	2.721	11.44	0.11	1.10	4.90
HC180F3D	0.25	1.08	1.37	0.258	4.006	9.755	0.038	4.034	9.534	0.11	1.77	4.32
HC180F3H	0.25	0.82	0.82	0.258	1.192	1.192	0.038	2.440	2.440	0.11	0.53	0.53
HC240F00	0.63	1.45	1.45	0.129	0.677	0.677	0.273	2.331	2.330	0.05	0.26	0.26
HC240F1D	0.63	2.04	2.16	0.129	1.659	2.913	0.273	2.485	6.015	0.05	0.65	1.14
HC240F3D	0.85	2.04	2.89	0.192	1.659	4.767	0.544	2.485	13.94	0.08	0.65	1.86
HC240F3H	0.63	1.46	1.46	0.129	1.461	1.461	0.273	1.352	1.352	0.05	0.57	0.57
HC280F00	0.34	0.99	1.13	0.120	2.626	7.424	0.076	2.431	6.455	0.05	1.03	2.90
HC280F1D	0.34	1.22	1.60	0.120	1.738	6.639	0.076	3.099	11.28	0.05	0.68	2.59
HC280F3D	0.65	1.47	2.14	0.260	1.872	11.01	0.519	2.559	12.81	0.10	0.73	4.30
HC280F3H	0.34	1.22	1.22	0.120	1.738	1.738	0.076	2.910	2.910	0.05	0.68	0.68
HC340F00	0.51	1.39	1.53	0.110	0.527	0.657	0.040	1.067	1.649	0.05	0.23	0.29
HC340F1D	0.63	2.04	2.12	0.373	2.943	5.457	0.193	4.034	11.66	0.17	1.30	2.41
HC340F3D	0.71	2.41	2.61	0.200	0.906	1.613	1.220	4.844	8.479	0.09	0.40	0.71
HC340F3H	0.66	1.32	1.36	0.126	0.425	0.425	0.037	0.267	1.615	0.06	0.19	0.19
HC380F00	0.33	0.79	0.79	0.196	1.434	1.563	0.078	1.908	2.211	0.09	0.63	0.69
HC380F1D	0.44	1.79	1.97	0.211	3.562	5.256	0.063	5.520	10.17	0.09	1.58	2.33
HC380F3D	0.52	2.25	2.46	0.269	3.966	5.786	0.269	7.321	13.71	0.12	1.75	2.56
HC380F3H	0.42	1.00	1.14	0.158	0.632	0.790	0.310	1.871	2.678	0.07	0.28	0.35
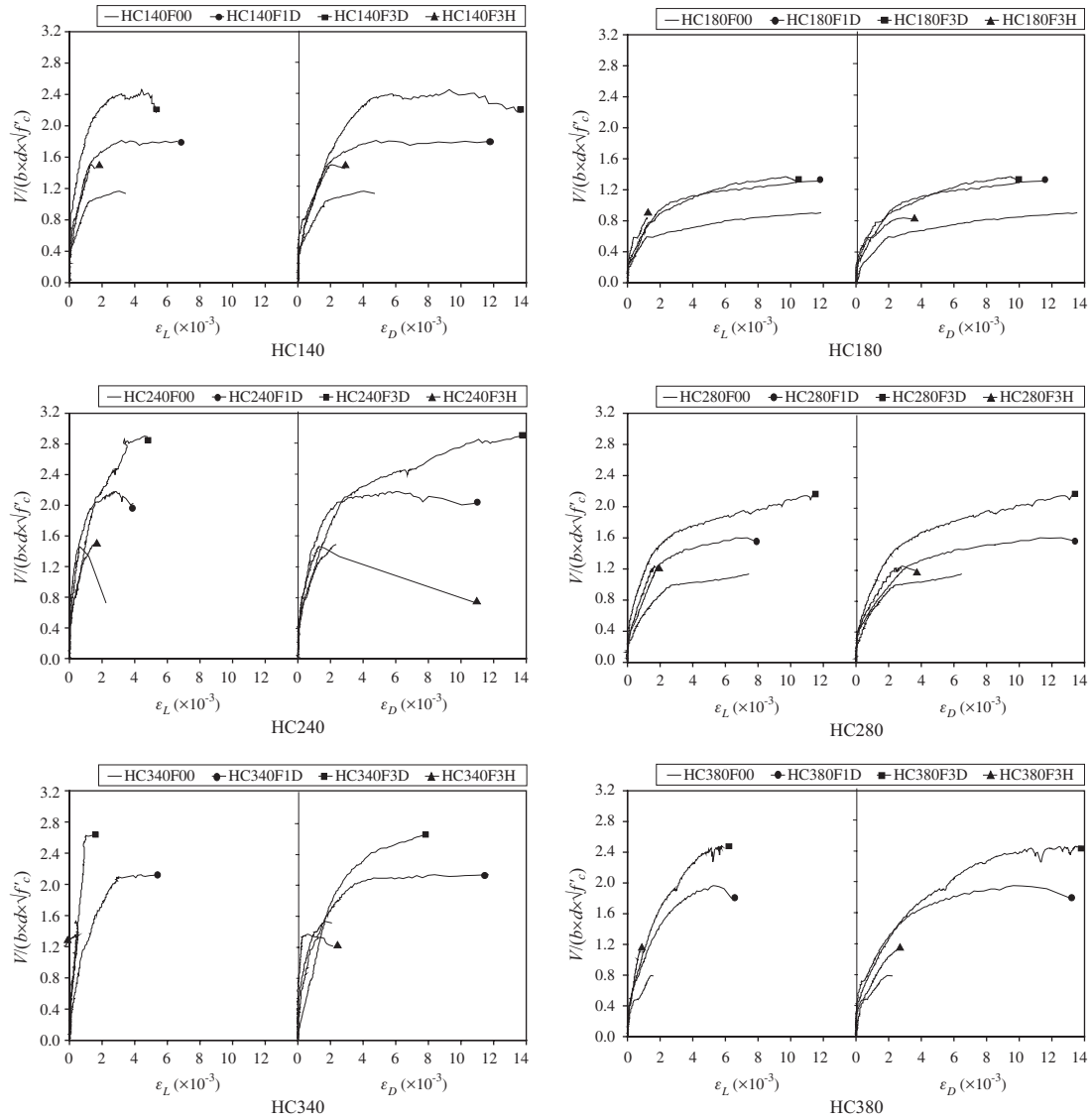
Figure 8   Normalized shear stress vs. lateral (ε_L) and diagonal (ε_D) strains.

GFRPs are generally above the yield strain for all specimens regardless of the *a/d* ratio, whereas the strains are adversely influenced by the increasing reinforcement ratios. It should be noted that the main reinforcements anticipated strains for the control specimens and the specimens strengthened with lateral GFRP overlays could not reach the yield values.

3.3. Failure modes

As previously mentioned, the test specimens were classified into three main groups according to the main reinforcement ratio and each group was divided into two subgroups according to the *a/d* ratios. Control specimens from each subgroup were tested to determine the load carrying capacity of the non-strengthened corbels. In all tests of the control specimens, the first visible crack was the flexural crack starting at or near the junction of the horizontal face of the corbel

and the neighboring face of the column as expected. Diagonal cracks were usually initiated at the load bearing point of the corbels and proceeded towards the intersection point of the inclined face of the corbel and the neighboring column face. The diagonal crack in the control specimens propagated more rapidly than the flexural crack did.

The control specimens with *a/d*=0.40 underwent compression strut failure (diagonal splitting), regardless of the reinforcement ratio (Figure 4). The failure pattern examined after testing revealed that the width of the failed concrete strut enlarged with the increase in the flexural reinforcement ratio. For control specimens with a higher *a/d* ratio (*a/d*=0.80) the failure type usually depends on the reinforcement ratio. For low reinforcement ratio (specimen HC180F00) the failure was a mix of flexural yielding at the junction (interface of the horizontal corbel face and the column neighboring face) and a proceeding diagonal tension initiated from the support point.

The failure of specimen HC180F00 took place when the main reinforcement yielded, resulting in a more ductile widening of the flexural crack. By contrast, a true diagonal splitting failure was observed for the highest reinforcement ratio specimen (HC380F00), spanning between the roller support and the column. The behavior of the HC280F00 specimen, which has an intermediate level of reinforcement ratio, experienced both flexural cracking and diagonal splitting, with diagonal splitting being the failure crack. Such a shift of failure type can be attributed to the big difference between the yield and ultimate strengths of the main reinforcement (Table 2).

It was observed that the crack forms in strengthened specimens were somewhat similar with the control specimens, especially for diagonal GFRP applications. By contrast, horizontal GFRP overlays caused an increased pseudo-reinforcement, and convert the flexural yielding of HC180F00 to a diagonal splitting in the counterpart specimen HC180F3H. In all specimens strengthened with horizontal GFRP overlays, the failure took place with the formation of the diagonal splitting crack.

4. Conclusions

The following conclusions are drawn from the results of the current experimental investigation.

- GFRP wrapping can be considered as an easy to apply and effective way to strengthen the reinforced concrete corbels.
- GFRP wrapping with 45 degree fiber orientation (diagonal) with regard to the corbel tension reinforcement yielded a higher degree of strengthening as compared to the wrapping with fibers parallel to the corbel tension reinforcement. Moreover, higher load capacities were experienced for higher numbers of diagonally applied GFRP layers.
- The failure pattern of the strengthened corbels is closely related to the GFRP fiber orientation. For wrappings parallel to the tension reinforcement of the corbel, the failure generally took place with the strut failure.
- The level of tension steel strain on the onset of failure usually depends on the type and number of layers of GFRP overlays along with the tension reinforcement ratio. For higher reinforcement ratios, smaller concrete strains were

observed, whereas higher strains were observed for higher a/d ratios.
- Test results revealed that the level of strengthening of corbels with GFRP wrapping ranges between 40% and 200%, depending on the reinforcement ratio of corbel, a/d ratio, and the orientation and number of layers of the GFRP overlay.

References

[1] Kriz LB, Raths CH. *PCI J.* 1965, 10, 16–61.
[2] Solanki H, Sabnis GM. *ACI Struct. J.* 1987, 84, 428–432.
[3] Fattuhi NI, Hughes BP. *ACI Struct. J.* 1989, 86, 590–596.
[4] Mattock AH, Chen KC, Soongswang K. *PCI J.* 1976, 31, 52–77.
[5] Fattuhi NI. *ACI Struct. J.* 1987, 84, 640–651.
[6] Fattuhi NI, Hughes BP. *ACI Struct. J.* 1989, 86, 644–651.
[7] Fattuhi NI. *J. Struct. Eng. ASCE* 1989, 120, 360–377.
[8] Fattuhi NI. *ACI Struct. J.* 1990, 116, 701–718.
[9] Fattuhi NI. *ACI Struct. J.* 1994, 91, 376–383.
[10] Abdul-Wahab MS. *ACI Struct. J.* 1989, 86, 60–66.
[11] Fattuhi NI. *ACI Struct. J.* 1994, 91, 530–536.
[12] Yong Y, Balaguru P. *J. Struct. Eng. ASCE* 1994, 120, 1182–1201.
[13] Foster SJ, Powell RE, Selim HS. *ACI Struct. J.* 1996, 93, 555–563.
[14] Triantafillou TC, Antonopoulos CP. *J. Compos. Constr. ASCE* 2000, 4, 198–205.
[15] Antonopoulos CP, Triantafillou TC. *J. Compos. Constr. ASCE* 2003, 4, 39–49.
[16] Elgwady MA, Rabie M, Mostofa MT. In *3rd International Conference for Composite in Infrastructure ICCI'02*, San Francisco, CA: USA, 2002.
[17] Campione G, La Mendola L, Papia M. *Mater. Struct.* 2005, 38, 617–625.